Available online at www.sciencedirect.com

ScienceDirect

Energy Procedia 148 (2018) 266–273

Energy Procedia

www.elsevier.com/locate/procedia

73rd Conference of the Italian Thermal Machines Engineering Association (ATI 2018), 12–14 September 2018, Pisa, Italy

Dynamic modelling of the swash plate of a hydraulic axial piston pump for condition monitoring applications

Andrea Bedotti[a], Mirko Pastori[a], Fabio Scolari[a], Paolo Casoli[a]*

[a]*University of Parma, Parco Area delle Scienze 181/A, Parma, 43124, Italy*

Abstract

In the last years Prognostic and Health Management (PHM) has become one of the challenging topic in the engineering field. In particular, model-based approach for diagnostic relies on the development of a mathematical model of the system representing its flawless status. Once the model has been developed and carefully calibrated on experimental data referred to flawless pump condition the comparison between the model output and the real system output leads to the residual analysis, which gives a diagnosis of the component health. This paper presents the mathematical model of a hydraulic axial piston pump developed in order to replicate the dynamic behavior of the swash plate for PHM applications. The model has been developed on the basis of simplified hypotheses, a friction model between swash plate and bearings has been introduced. A detailed experimental activity was carried out to calibrate and validate the model with step tests and sweep tests. The comparison between numerical and experimental results shows a satisfying agreement and highlights the model capability to reproduce the swash plate dynamics. Future works will include tests with the pump in faulty conditions to evaluate the pump health state through the residual analysis of the swash plate position.

Keywords: Axial Piston Pump; Dynamic modelling; Friction model; Condition Monitoring.

* Corresponding author: *E-mail address:* paolo.casoli@unipr.it

1876-6102
10.1016/j.egypro.2018.08.077

1. Introduction

Nowadays, prognostics and health management is rapidly gaining interest from both academia and industry. Most of the efforts have led to the development of diagnostics methodologies which can increase the reliability and safety of the machine. The purpose is that of determine the system health state and detect or identify an incipient fault before a system breakdown occurs. Preventive and scheduled maintenance can be eliminated enabling a real time monitoring with the result of significant cost savings and downtime reduction. Different approaches were used to the diagnostic of the hydraulic systems: data-driven, model-based and hybrid diagnostic approaches. Data driven concept is based on data acquired from the system for the development of diagnostic algorithm. The data-driven approaches consist of an offline phase for the training of a classification algorithm and an online phase when the system is operating, to compute the diagnosis. Furthermore, diagnostic solutions have been conceived for hydraulic components and systems. Gao et al. [1] applied on the delivery pressure signal of a hydraulic pump the wavelet analysis while a vibration-based methodology, through the testing of different classifiers, was conceived by Torrika et al. [2]. Buono et al. [3,4] applied a vibration analysis to detect abnormal working conditions for a gerotor pump. Casoli et al. [5] proposed the thermodynamic method based on temperature measurements as condition monitoring tool for axial piston pumps. Some works involve the development of PHM solutions for the overall hydraulic system. Campanini et al. [6] presented an optimized control with diagnostic features for an independent metering hydraulic system; Helwig et al. [7] tested a novel condition monitoring approach based on Linear Discriminant Analysis to detect the system degradation. El-Betar et al. [8] developed a diagnostic tool for the identification of actuator internal leakage and valve blockage based on artificial neural network. On the other side, model-based approach exploits data generated from an accurate model of the system in healthy conditions; the comparison between real data and mathematical model outputs permits the faults detection. The difference between the model output and the real system output is the so-called residual. The analysis of the residuals can be performed not only for the fault detection but also for the identification; indeed, each fault can affect residual values in a different combination. Medjaher et al. [9] presented the model of a hydraulic circuit where the diagnosis is computed by analysing the residual values. Palazzolo et al. [10] proposed the use of a physics-based model for the detection of different types of leakages in a variable displacement axial-piston pump installed on an aircraft. A hybrid approach between data driven and model-based was presented by Marcu et al. [11] which exploited dynamic neural networks to simulate the behavior of different systems; the classifier is trained referring to past data and then applied online to create residuals for the diagnosis. In literature, different modelling approach can be found with the purpose of analyse solutions for efficiency improvements [12-17], conduct energy analysis for both systems and components [17-18], optimize the power split transmission [20-22] or the coupling between the engine and the hydraulic system [23] and support the designer during the prototype development [24-27].

In this work, a mathematical model of the swash plate of an axial piston pump has been developed for diagnostic purpose. Axial piston pumps with variable displacement are widely used in industry as hydraulic transfer device thanks to fast response time and power economy. During the last decades significant researches have been conducted to study the static and dynamic behavior of swash plate axial piston pumps. Zeiger et al. [28] and Lin [29] presented a comprehensive mathematical model for the estimation of the average torque on the swash plate for steady state conditions; Schoenau et al. [30] proposed a dynamic model of the pump and found a good correlation between experimental and theoretical transient responses. The contribution of this work is that of modelling accurately the swash plate dynamics considering all the torque contributions acting on the swash plate and of developing a reliable tool for condition monitoring applications. This work involves the modelling of pump regulators and considers the friction between swash plate and bearings. Experimental step and sweep tests have permitted to calibrate and validate the model. The next step of the research activity will be the testing of the pump in faulty conditions to evaluate the effects of failures on the acquired signals and develop a methodology based on the residual analysis between model and real system outputs.

2. Mathematical model

2.1. Kinematic analysis

Considering the geometric characteristics of the pump, the equation of the instantaneous piston displacement is a function of the swash plate angle and of the rotation angle of cylinder block, eq. (1). Figure 1 shows the representation of the cylinder block and a single piston coupled with a slipper and the swash plate to deduce the piston displacement. The swash plate is inclined by an angle α respect the vertical axis. Furthermore, through this scheme can be defined: the circular position of the piston with respect to the y-axis (ϑ) and the piston-pitch radius (R). In the right side view of fig. 1, the rotational axis of the swash plate is identified with a yellow spot; respect to the rotational axis of the cylinder block there is an eccentricity e.

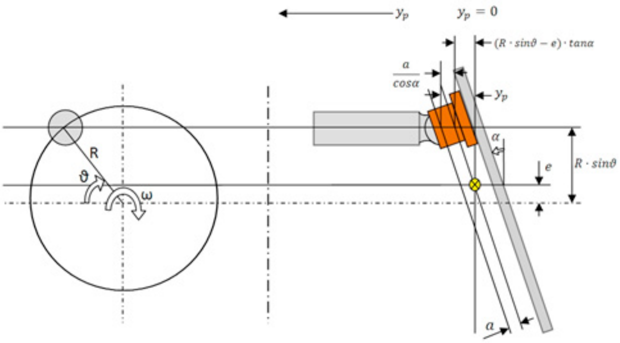

Fig. 1. Scheme of the pump kinematics

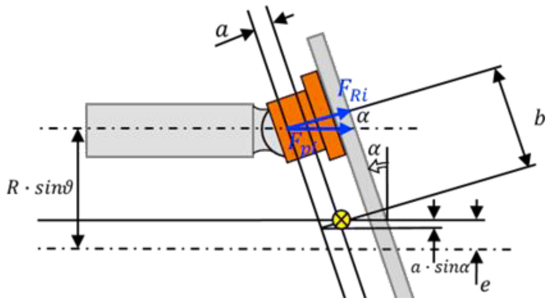

Fig. 2. Scheme of the piston forces acting on the swash plate

The piston displacement y_p is calculated by eq. (1); after deriving eq. (1), the piston speed can be obtained, eq. (2):

$$y_p = \frac{a}{\cos\alpha} + R \cdot \sin\vartheta \cdot \tan\alpha - e \cdot \tan\alpha \quad (1)$$

$$\dot{y}_p = \left(\frac{R \cdot \sin\vartheta + a \cdot \sin\alpha - e}{cos^2\alpha}\right) \cdot \dot{\alpha} + +R \cdot \omega \cdot \cos\vartheta \cdot \tan\alpha \quad (2)$$

Further deriving, eq. (2), the acceleration of the piston is found:

$$\ddot{y}_p = -\omega^2 \cdot R \cdot \sin\vartheta \cdot \tan\alpha + \left(\frac{2 \cdot \omega \cdot R \cdot \cos\vartheta}{cos^2\alpha}\right) \cdot \dot{\alpha} + \left[\frac{a\,(cos^2\alpha + 2 \cdot sin^2\alpha) + 2 \cdot R \cdot \sin\alpha \cdot \sin\vartheta - 2 \cdot e \cdot sin\alpha}{cos^3\alpha}\right] \cdot \dot{\alpha}^2 + \left(\frac{R \cdot \sin\vartheta + a \cdot \sin\alpha - e}{cos^2\alpha}\right) \cdot \ddot{\alpha} \quad (3)$$

2.2. Equation of motion

The equilibrium position of the swash plate depends on the forces that each component of the pump applies on the swash plate. On the swash plate different torques act due to: the forces exerted by the pumping elements (F_p); the force exerted by the cylinder block spring (F_k); the force exerted by the displacement actuator control (F_{act}).

To evaluate the equilibrium position reached, the equation of dynamic equilibrium that yields to eq. (4) is used.

$$J \cdot \ddot{\alpha} + T_f = \sum_{i=1}^{9} T_{p\,i} + T_m - T_{act} \quad (4)$$

Where: T_{pi} is the torque exerted by i-th piston, T_m is the torque exerted by the spring, T_{act} is the torque exerted by the actuator control, J is the overall mass moment of inertia of the swash plate, slipper and slipper hold-down and T_f is the friction torque. Rearranging eq. (4), the acceleration of the swash plate can be deduced:

$$\ddot{\alpha} = \frac{\sum_{i=1}^{9} T_{p\,i} + T_m - T_{act} - T_f}{J} \quad (5)$$

The torque exerted by the i-th piston can be evaluated with eq. (6) starting from the forces generated by the pistons, fig.2:

$$T_{p\,i} = F_{Ri} \cdot b_i \quad (6)$$

Where the force F_{Ri} is defined with eqs. (7,8) for the i-th piston and the piston force moment-arm (b_i) is calculated for each piston with eq. (9).

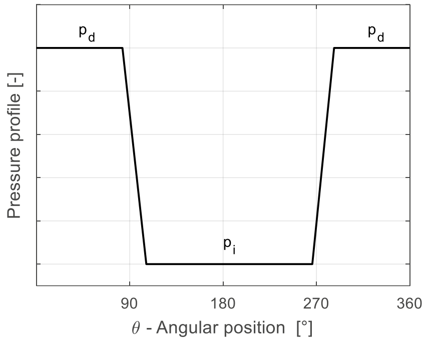

Fig. 3. Pressure profile

$$F_{p\,i} = -\left(M_p \cdot \ddot{y}_{p\,i} + f \cdot \dot{y}_{p\,i} + p \cdot A_p\right) \quad (7)$$

$$F_{R\,i} = \left[\frac{F_{p\,i}}{cos\alpha}\right] \quad (8)$$

$$b_i = \frac{R \cdot sin\vartheta_i - e + a \cdot sin\alpha}{cos\alpha} \quad (9)$$

In eq. (7) M_p is the piston mass, p is the fluid pressure acting on the piston and A_p is the piston area, while the term f is expressed by eq. (10), [30]:

$$f = \frac{\mu \cdot \pi \cdot \frac{d_p}{2} \cdot (L_p + y_p)}{h_p/2} \quad (10)$$

Where: d_p is the piston diameter, L_p is the minimum length of contact between piston and relative chamber and h_p is the radial clearance between piston and guide, μ is the fluid dynamic viscosity.

In this work, it has been assumed a simplified approach to evaluate the pressure inside the chamber of each piston. The pressure profile that acts on the pistons has been obtained through geometrical consideration and it can be observed in fig. 3, for both inlet (p_i) and delivery pressure (p_d) average value.

The force exerted by the spring located inside the cylinder block introduces a torque on the swash plate due to the eccentricity e, fig. 1: $T_m = F_k \cdot e$.

Finally, the torque imposed by the control displacement actuator is controlled by the actuator pressure that is calculated by the mathematical model of the regulator.

2.3. Karnopp Model

The coupling between the swash plate and the bearings has been modelled with the Karnopp friction model. This model permits to define the static and viscous friction depending on the swash plate velocity [31]. The Karnopp model defines a speed interval equal to $\dot{\alpha}_{th}$; if the velocity is smaller than $\dot{\alpha}_{th}$, the model considers the swash plate velocity equal to zero. In this speed interval the friction torque has been set equal to the minimum value between the torque acting on the swashplate (T_{tot}) and the maximum static friction torque (Ts_{max}).

After this region there is a descendent line due to Stribeck effect and then an increase of the torque owing to viscous friction, eq. (11). The Karnopp coefficients reported in table 1 have been defined in order to match the simulated results with experimental data.

$$(11)\begin{cases} T_f = \min(|T_{tot}|, Ts_{max}) \cdot sign(T_{tot}) & \dot{\alpha} < \dot{\alpha}_{th} \\ T_f = \left(T_c + \left((Ts_{max} - T_c) \cdot e^{(-C_v|\dot{\alpha}|)}\right)\right) \cdot sign(\dot{\alpha}) + C \cdot \dot{\alpha} & \dot{\alpha} > \dot{\alpha}_{th} \end{cases}$$

Table 1. Karnopp model coefficients

Viscous friction coefficient C $[N \cdot m \cdot s\,/rad]$	50
Coulombian torque T_c $[N \cdot m]$	10
Static torque Ts_{max} $[N \cdot m]$	48
Stribeck coefficent C_v $[s/rad]$	100

2.4. Flow Compensator

The flow compensator (FC) has the important function of maintaining a fixed differential pressure across the control orifice by modulating the pump displacement. The logic integrated in the FC is to compare the load sensing pressure (p_{LS}) with the pump delivery pressure (p_d) to modulate the torque exerted by the actuator control (T_{act}) . The mathematical model of the compensator includes a fluid-dynamic model and a mechanical-geometrical model. The fluid-dynamic model is based on a lumped parameter framework. The pressure inside each control volume is assumed uniform and time dependent and is determined by means of the pressure-rise rate equation combining the continuity and fluid state equations and assuming constant fluid temperature. The mechanical model calculates the instantaneous position and velocity of the spool using Newton's second law; the forces acting on the spool of the compensator considered are: hydrostatic forces; spring force; friction forces; hydrodynamic forces [12].

2.5. Theoretical pressure and flow rate delivered by the pump

The flow rate delivered by the pump has been calculated as a sum of the flow delivered by each piston eq. (12), considering the leakages between piston and cylinder :

$$Q_i = \dot{y}_{pi} \cdot A_p - \frac{\pi \cdot r_p \cdot {h_p}^3}{6 \cdot \mu \cdot (L_p + y_{pi})} \cdot \Delta p \qquad Q_{tot} = \sum_{i=1}^{9} Q_i \quad (12) \qquad Q_{tot} = C_d\, \Omega \sqrt{\frac{2\,|p_d - p_{LS}|}{\rho}} \quad (13)$$

With reference to fig. 4 the load sensing pressure has been assumed as an input of the model, while the delivery pressure has been calculated by means of the orifice equation (eq. 13) assuming steady-state conditions:

The orifice equation defines a correlation between the delivery pressure, flow rate and flow area (Ω). In transient conditions a sudden change in the flow area changes the value of the pressure drop (pump margin) until the pump sets the flow rate at the new value. The model assumes a quasi steady-state conditions during the transient and the delivery pressure so defined has been used to estimate the pressure actuator through the mathematical model of the flow compensator.

3. Experimental activity

A wide experimental activity was carried out with the aim of calibrating and validating the pump mathematical model. The tests were performed on the test bench installed at the Laboratory of the Engineering and Architectural Department at the University of Parma. The case study is the variable displacement axial piston pump Casappa® MVP60-84. The pump is equipped with a Flow compensator (FC) and with a Pressure compensator (PC) and is installed in Load Sensing (LS) circuit. The FC regulates the pump displacement to keep a constant pressure drop (pump margin) between the LS pressure and the pump delivery pressure. The PC acts to limit the pump displacement when the delivery pressure reaches the maximum tolerable value (280 bar in this application). The flow rate is controlled with a proportional valve installed in the delivery line as well as the LS pressure is controlled with another proportional valve. The pump was instrumented with several sensors in order to acquire: suction fluid temperature, delivery pressure, swash plate angular position, torque, shaft speed, delivery flow rate and drain flow rate. The hydraulic scheme of the experimental layout is reported in Fig. 4.

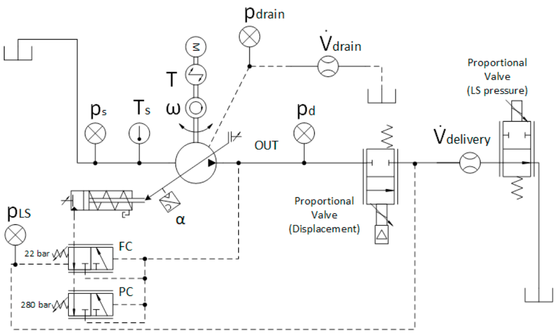

Fig. 4. Hydraulic scheme of the experimental layout

Table 2. Transducers type and features

Variable	*Sensor*	*Main Features*
Ts	Thermistor Pt100	0 – 100 °C ±0.2 °C
Ps	Pressure Transducer	0 – 10 bar ±0.3%FS
p_d, p_{LS}	Pressure Transducer	0 – 400 bar ±0.5%FS
$\dot{V}_{delivery}$	Flow Meter	0.1-150 l/min ± 0.3% measured value
$\dot{V}_{drain}$	Flow Meter	0.01-80 l/min ± 0.3% measured value
α	Angular sensor	0° – 360° ± 0.02°
ω	Speed sensor	accuracy class 0.05

In order to understand the behavior of the pump in transient conditions, two different types of dynamic tests were performed: step and sine sweep displacement tests. In all the tests, the displacement was modified by moving the proportional valve spool, keeping the angular velocity and the delivery pressure constant. The proportional directional valve installed has a response time less than 20 ms. For each test, the data were acquired with a sampling frequency of 1000 Hz. Step tests were executed under different conditions of delivery pressure and rotation speed by repeating the same step up and step down several times, in order to verify the repeatability of the data. Sine sweep tests were carried out keeping constant amplitude and varying the frequency.

4. Model validation and Experimental results

The swash plate mathematical model implements the Karnopp friction model whose coefficients have to be calibrated with experimental data. As reported in fig. 5 the first simulated results, with a preliminary setting of the friction coefficients with values found in literature, are not satisfying for the purpose of the model. The dynamic response of the model is slower if compared with the measured data. In order to calibrate the coefficients of the model has been used a Matlab's tool called Parameter Estimation; this tool is able to estimate the parameters solving an optimization problem, reaching the best possible fitting between the simulation results and experimental measurements. After the optimization process the simulation results show a satisfying prediction of the swash plate dynamic, fig.5. The time line has been divided for a reference time for confidential reasons.

In fig. 6 is presented the friction torque at different values of swash plate speed according to the Karnopp model, before and after the optimization process.

After the parameters optimization, the model has been further tested providing different step tests in different working conditions. Analysing the case reported in fig. 7 respect that reported in fig. 8 appears a discrepancy during the step up phase between the experimental data and the simulation results when the valve is adjusting to a higher extend fig.7, while to lesser extend fig. 8 the model follows perfectly the real behaviour of the pump.

In fig. 9 is reported a case at lower speed and also at this working condition the model is able to predict the swash plate angle course in satisfactory manner. The step down phases are simulated in good manner for each performed test.

In order to validate the model sweep tests have been conducted. In a sweep test, the frequency of the sinusoidal law applied to the spool opening linearly increases with time. Figure 10 shows two windows of a sweep test; in fig. 10(b) the frequency is triple than in fig. 10(a) and in both case the simulation results are satisfying. Future development of the model will be carried out in the path of developing a condition monitoring based on a model-based approach. A critical aspect is the coupling swash plate-bearings; further experiments will permit to verify and define in more accurate manner the Karnopp coefficients.

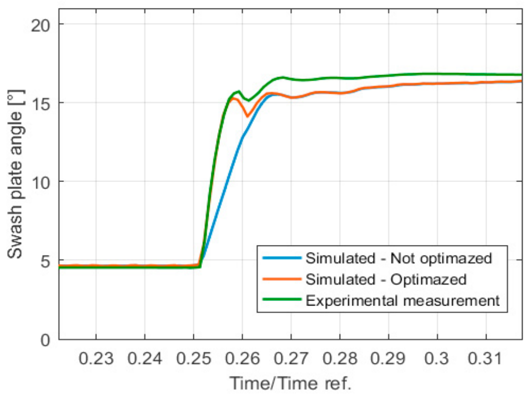

Fig. 5 Step Test: 1500 rpm, p_d =150 bar, spool opening 23-48%

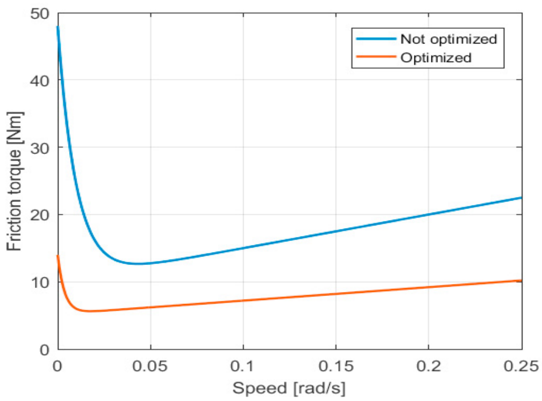

Fig. 6 Friction torque according to Karnopp model

As described the model does not simulate fluid dynamic effects; cylinder pressure is considered constant and equal to the average delivery pressure. A further research activity will be focused on a detailed experimental and numerical analysis of the dynamic response of the flow compensator that controls the swash plate actuator. The flow compensator receives the delivery pressure as input signal and the hypothesis of assuming a constant delivery pressure will be further investigated. Finally, the authors will carry out experimental tests on flawless and faulty pumps to define a methodology for fault detection and identification.

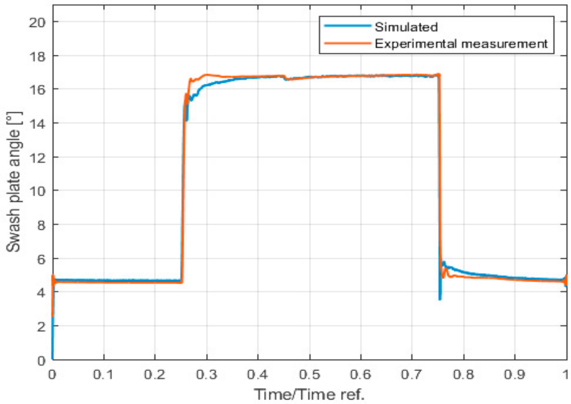

Fig. 7 Step Test: 1500 rpm, pd =150 bar, spool opening 23-48%

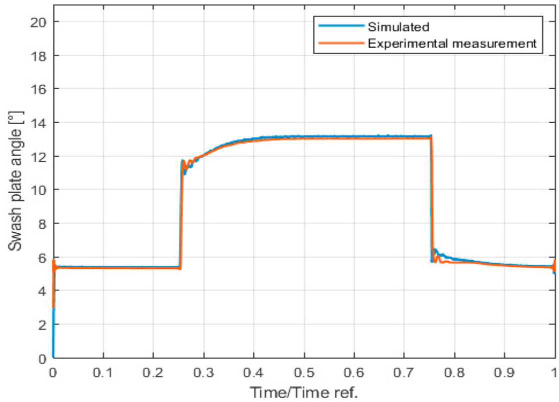

Fig. 8 Step Test: 1500 rpm, pd =150 bar, spool opening 25-44%

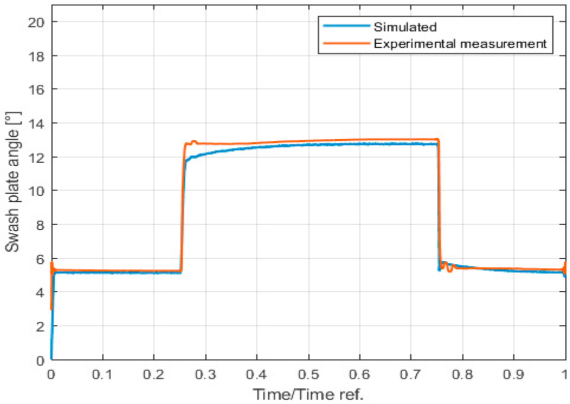

Fig. 9 Step Test: 1000 rpm, pd =50 bar, spool opening 17-35%

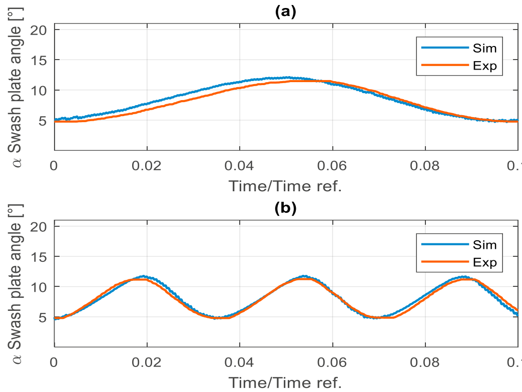

Fig. 10 Sweep Test: 1000 rpm, pd =50 bar

4. Conclusions

In this paper a mathematical model of an axial piston pump to predict the dynamic response of the swash plate for condition monitoring applications has been presented. The model is based on the equation of motion of the swash plate; pump regulators have been modelled to define the actuator torque and the Karnopp friction model has been introduced to model the coupling between the swash plate and the bearings. Step and sweep tests were carried out to provide experimental data, to calibrate and to verify the model; in particular the Karnopp coefficients were defined through a parameter estimation process. The comparison between numerical and experimental results reveals a satisfying agreement between curves. Future works will include tests with the pump in faulty conditions in order to define a model-based approach to monitor in real-time the pump state.

References

[1] Gao Y., Zhang Q., A Wavelet Packet and Residual Analysis Based Method for Hydraulic Pump Health Diagnosis, Proceedings of the Institution of Mechanical Engineers, Part D: Journal of Automobile Engineering, Vol. 220 (2006), issue 6, pp: 735-745 [2]

[2] Torikka T., Evaluation of Analysis Methods for Fault Diagnosis, The Twelfth Scandinavian International Conference on Fluid Power, May 18-20, 2011, Tampere, Finland.

[3] D. Buono, D. Siano, E. Frosina, A. Senatore, 2017, Gerotor pump cavitation monitoring and fault diagnosis using vibration analysis through the employment of auto-regressive-moving-average technique, In Simulation Modelling Practice and Theory, Volume 71, 2017, Pages 61-82, ISSN 1569-190X

[4] E. Frosina, A. Senatore, D. Buono, K. A. Stelson, F. Wang, B. Mohanty, M. J. Gust, 2015, Vane pump power split trasmission: three dimensional computational fluid dynamic modeling, Proceedings of the ASME/BATH 2015 Symposium on Fluid Power and Motion Control, FPMC2015, Chicago, Illinois, USA, DOI: 10.1115/FPMC2015-9518, Scopus Code: 2-s2.0-84964330332.

[5] Casoli, P., Campanini, F., Bedotti, A., Pastori, M., Lettini, A. Overall Efficiency Evaluation of a Hydraulic Pump with External Drainage Through Temperature Measurements (2018) Journal of Dynamic Systems, Measurement and Control, Transactions of the ASME, 140 (8), art. no. 081005. DOI: 10.1115/1.4039084
[6] Campanini F., Bianchi R., Vacca A., Casoli P., Optimized control for an independent metering valve with integrated diagnostic features, Proceedings of the ASME/BATH 2017 Symposium on Fluid Power & Motion Control, October 16-19, 2017, Sarasota, Florida, USA. DOI:10.1115/FPMC2017-4302
[8] El-Betar A., Abdelhamed M., El-Assal A., Abdelsatar R., Fult Diagnosis of a Hydraulic Power System Using an Artificial Neural Network, JKAU: Eng. Sci., Vol. 17 (2006), No. 1, pp: 117 – 137.
[7] Helwig N., Pignanelli E., Schütze A., Condition Monitoring of a Complex Hydraulic System using Multivariate Statistics, Instrumentation and Measurement Technology Conference (I2MTC), May 11-14, 2015, Pisa, Italy.
[9] K. Medjaher, N. Zerhouni, Residual-based failure prognostic in dynamic systems, Proceedings of the 7th IFAC Symposium on Fault Detection, Supervision and Safety of Technical Processes Barcelona, Spain, June 30 - July 3, 2009.
[10] J. J. Palazzolo, L. D. Scheuemann, J. R. Hartin, Leakage Fault Detection Method for Axial-Piston Variable Displacement Pumps, Aerospace Conference, 2008 IEEE, 1-8 March 2008, Big Sky, MT, USA.
[11] T. Marcu, B. Köppen-Seliger, R. Stücher, Design of fault detection for a hydraulic looper using dynamic neural networks, Control Engineering Practice 16 (2008) 192–213.
[12] Casoli, P.; Gambarotta, A.; Pompini, N.; Riccò, L. Hybridization methodology based on DP algorithm for hydraulic mobile machinery—Application to a middle size excavator. *Automation in Construction* Volume 61, January 2016, Pages 42–57. doi:10.1016/j.autcon.2015.09.012.
[13] Casoli, P.; Anthony, A.; Rigosi M.; Modeling of an Excavator System – Semi empirical hydraulic pump model SAE 2011 Commercial Vehicle Engineering Congress, Rosemont, Illinois, USA, 13-14 September 2011. doi:10.4271/2011-01-2278.
[14] Casoli, P.; Anthony, A.; Riccò, L.; Modeling simulation and experimental verification of an excavator hydraulic system—Load sensing flow sharing valve model. In Proceedings of the SAE 2012 Commercial Vehicle Engineering Congress, doi:10.4271/2012-01-2042.
[15] Casoli, P.; Pompini, N.; Riccò, L.; Simulation of an Excavator Hydraulic System Using Nonlinear Mathematical Models; *Strojniški vestnik - Journal of Mechanical Engineering* 61(2015)10, 583-593, doi:10.5545/sv-jme.2015.2570.
[16] Casoli, P.; Gambarotta, A.; Pompini, N.; Riccò L.; Development and application of co-simulation and control-oriented modeling in the improvement of performance and energy saving of mobile machinery", *Energy Procedia*, http://dx.doi.org/10.1016/j.egypro.2014.01.090
[17] Casoli, P.; Riccò, L.; Campanini, F.; Lettini, A.; Dolcin, C.; Mathematical model of a hydraulic excavator for fuel consumption predictions. In Proceedings of the ASME/BATH 2015 Symposium on Fluid Power and Motion Control, Chicago, USA, 2015. doi:10.1115/FPMC2015-9566
[18] Pintore F., Borghi M., Morselli R., Benevelli A., Zardin B., Belluzzi F.; Modelling and Simulation of the Hydraulic Circuit of an Agricultural Tractor. ASME. Fluid Power Systems Technology, 8th FPNI Ph.D Symposium on Fluid Power; V001T04A004. doi:10.1115/FPNI2014-7848.
[19] Casoli, P.; Riccò, L.; Campanini, F.; Bedotti A. ;Hydraulic Hybrid Excavator—Mathematical Model Validation and Energy Analysis. *Energies MDPI* 2016, 9, 1002; doi:10.3390/en9121002
[20] Casoli P., Vacca A., G.,Berta, Meleti S., Vescovini M. (2007) A numerical model for the simulation of Diesel/CVT power split transmission, SAE paper n. 2007-24-137, SAE-NA ICE2007, 17-20 Settembre, 2007 Capri-Napoli. ISBN: 978-88-900399-3-0. DOI: 10.4271/2007-24-0137
[21]Rossetti A., Macor A., Scamperle M. "Optimization of components and layouts of hydromechanical transmissions"International Journal of Fluid Power Volume 18, Issue 2, 4 May 2017, Pages 123-134. DOI: 10.1080/14399776.2017.1296746. Codice Scopus:2-s2.0-85015076287
[22] Macor A., Rossetti A., Scamperle M. "Prediction of sound pressure level for a dual-stage hydromechanical transmission". International Journal of Fluid Power, Volume 17, Issue 1, 2 January 2016, Pages 25-35. DOI: 10.1080/14399776.2015.1120137. Codice Scopus: 2-s2.0-84958945379.
[23] Casoli P., Gambarotta A., Pompini N., Riccò L.; Coupling excavator hydraulic system and internal combustion engine models for the real-time simulation; *Control Engineering Practice*, 2015, pp. 26–37 http://dx.doi.org/10.1016/j.conengprac.2015.04.003.
-[24] A. Senatore, D. Buono, E. Frosina, L. Santato, 2013, "Analysis and Simulation of an Oil Lubrication Pump for the Internal Combustion Engine". In: Fluids Engineering Systems and Technologies. San Diego, 15-21 November 2013ASME, Proceedings (IMECE) vol. 7B, ISBN/ISSN: 9780791856321, doi: 10.1115/IMECE2013-63468, Scopus Code= 2-s2.0-84903476543.
-[25]Altare G., Rundo M. "Advances in simulation of gerotor pumps: An integrated approach", Proc. IMechE Part C: J. Mechanical Engineering Science 231(7): 1221-1236, 2017. DOI: 10.1177/0954406217694663. Scopus: 2-s2.0-85016261465. WOS: 000398206700003
[26] Altare G., Rundo M.. "CFD Analysis of gerotor lubricating pumps at high speed: geometric features influencing the filling capability", Proceedings of the ASME/BATH 2015 Symposium on Fluid Power and Motion Control (FPMC), Oct. 12-14, 2015, Chicago, IL, USA. Paper no. FPMC2015-9539. DOI: 10.1115/FPMC2015-9539. Scopus: 2-s2.0-84964403756.
[27] Borghi, M.; Specchia, E.; Zardin, B.; Corradini, E.;The Critical Speed of Slipper Bearings in Axial Piston Swash Plate Type Pumps and Motors. ASME. Dynamic Systems and Control Conference, ASME 2009 Dynamic Systems and Control Conference, Volume 1:267-274. doi:10.1115/DSCC2009-2604.
[28] Zeiger GG, Akers AA. Torque on the Swashplate of an Axial Piston Pump. ASME. *J. Dyn. Sys., Meas., Control.* 1985;107(3):220-226. doi:10.1115/1.3140724.
[29] 8 Lin, S., Akers, A., and Zeiger, G., Oil Entrapment in an Axial Piston Pump and its Effect Upon Pressures and Swashplate Torques, *Proceedings of the 42nd National Conference on Fluid Power,* Chicago, Mar. 1987, pp. 113-124.
[30] Schoenau GJ, Burton RT, Kavanagh GP. Dynamic Analysis of a Variable Displacement Pump. ASME. *J. Dyn. Sys., Meas., Control.* 1990;112(1):122-132. doi:10.1115/1.2894129.
[31] Rodrigo A. R., C. Garcia, Karnopp friction model identification for a areal control valve, Proceedings of the 17th World Congress IFAC, The International Federation of Automatic Control Seoul, Korea, July 6-11, 2008.